A study on VPO specimen supported on aluminum-containing MCM-41 for partial oxidation of *n*-butane to MA

Weiyan Nie [a], Xiaoshu Wang [b], Weijie Ji [a,*], Qijie Yan [a], Yi Chen [a] and C.T. Au [c]

[a] *Department of Chemistry, Nanjing University, Nanjing 210093, PR China*
[b] *Center for Material Analysis, Nanjing University, Nanjing 210093, PR China*
[c] *Department of Chemistry, Hong Kong Baptist University, Hong Kong, PR China*

Received 18 May 2001; accepted 19 July 2001

Dispersed vanadium–phosphorus oxide species supported on Al-MCM-41 with different vanadium loadings have been synthesized for the first time for the partial oxidation of butane to MA. It was found that the VPO species was dispersed over the Al-MCM-41 support material, both in the internal channel and on the external surface. With increasing vanadium loading, *n*-butane conversion increased but MA selectivity decreased considerably under the same reaction conditions. At lower conversions (<30%), rather high MA selectivity (*ca.* 70%) can be achieved on the low loading sample. Compared with the amorphous structure of large pore SiO_2 support, the unique structure of the MCM-41 and the incorporated Al^{3+} in the framework do have an impact on the reaction behavior of the supported VPO specimen. The chemical nature of the supported VPO species and the interaction between the applied VPO species and the support was found to vary notably with the content of vanadium in the sample and likewise affected the related physico-chemical characteristics and their reaction behaviors.

KEY WORDS: Al-MCM-41; supported VPO catalysts; butane oxidation; maleic anhydride

1. Introduction

Currently, the selective oxidation of butane to maleic anhydride (MA) is the only commercially practiced chemical process for light paraffins [1]. The catalyst used for this reaction consisted primarily of unsupported vanadyl pyrophosphate, $(VO)_2P_2O_7$. Supported catalysts, however, offer several potential advantages over their unsupported counterparts: (1) increased surface area to volume ratio of the active phase, (2) increased mechanical strength and (3) improved heat transfer characteristics. Although many researchers have attempted to prepare supported vanadium–phosphorus oxide (VPO) catalysts on SiO_2, TiO_2, Al_2O_3, *etc.* [2–6], the use of a support introduces support–oxide interactions that might hinder the formation of the VPO phases. The resulting materials generally consisted of a phase that strongly resembles V^{5+} phosphate, mostly α-$VOPO_4$ or γ-$VOPO_4$ [7,8], and exhibited low butane conversion and MA selectivity. Birkeland *et al.* reported that the SiO_2 supported VPO catalysts showed *ca.* 50% selectivity to MA, with butane conversion less than 20% [2].

In many studies, it was revealed that the deposition of a VPO species onto a support material yielded intriguing capabilities, and application of different support materials could give an insight in understanding the complicated properties of VPO catalysts. It was found that when VPO species strongly interacted with a reducible support, such as titania and zirconia, it will become more reducible, which remarkably enhanced the catalytic activity. On the other hand, application of a support material, such as silica, which differently and less strongly interacted with the applied active phase/species, enhanced the selectivity but decreased the conversion [3,4].

For this reaction, it is known that the selectivity is mainly determined by two variables: (1) the sequential or consecutive oxidation of maleic anhydride influenced by internal mass-transport limitation; and (2) the parallel oxidation of *n*-butane to its total oxidation products, which is determined by the reactivity and the amount of oxygen species taking part in the reaction. Internal mass-transport limitation can be decreased to a certain degree by applying a support material with wider pores, therefore, the ordered mesoporous materials of the MCM-41 type are selected as the supports in this study, which consist of an ordered hexagonal array of pores (ranging from 20 to 100 nm). These materials, first developed by Mobil researchers [9,10], are basically the solids made of SiO_4 tetrahedra in which Al or other metal [11] can substitute some of Si atoms. These solids can have a high thermal stability (up to 900 °C), a large surface area (more than 700 m^2/g) and mild surface acidity [12]. Due to these unique features, supporting VPO species onto this type of material may yield interesting information and has not been investigated yet so far. It was reported in literature that the increased surface acidity favored desorption of partially oxidized products with acidic features, such as maleic anhydride, resulting in an improvement in MA selectivity [13]. For this consideration, certain amount of aluminum was incorporated into the framework of MCM-41 to modify the surface acidity of the support material [14]. A series of VPO specimen supported on Al-containing MCM-41 (Si/Al ratio = 30) with different loading of vanadium

* To whom correspondence should be addressed.

1011-372X/01/1000-0201$19.50/0

(2.7–18.6 wt%) were synthesized and characterized by the techniques including BET, XRD, TEM, XPS, TPR, *etc*. and evaluated for partial oxidation of *n*-butane to MA. Here we reported the results obtained.

2. Experimental

2.1. Preparation of mesoporuos Al-containing MCM-41 materials

For this study, the synthesis of Al-containing MCM-41 materials (Si/Al = 30) was based on the procedure detailed in [10], which involved mixing sodium silicate and cetyltrimethylammonium bromide (CTAB) as the template.

Briefly, a gel with a molar composition of $SiO_2 : 0.016\ Al_2O_3 : 0.25CTAB : 60H_2O$ was prepared by using $NaSiO_3 \cdot 6H_2O$ as the silicon source, CTAB (25 wt% solution in water) as the surfactant, NaOH as basic source and $NaAlO_2$ served as the aluminum source. The pH of the gel was adjusted to *ca.* 9.6. Crystallization of the gel was carried out in a Teflon-lined stainless-steel autoclave at 413 K for 28 h. After that the resulting solid product was recovered by filtration, washed with deionized water and dried in air at ambient temperature. The as-synthesized product was granulated and calcined at a rate of 1 K/min from room temperature to 823 K in flowing nitrogen, kept at this temperature for 1 h, followed by 6 h in flowing air.

2.2. Preparation of the MCM-41 supported VPO catalyst precursors

In this study, 5, 20 and 35 wt% VPO loadings correspond to vanadium content of 2.7, 10.6 and 18.6 wt%, respectively.

As an example, the 20 wt% VPO/Al-MCM-41 catalyst precursor was prepared in organic medium by employing the reaction of vanadium pentoxide (V_2O_5, 0.36 g) with a mixture of isobutanol (20 ml) and benzyl alcohol (20 ml). After the reaction mixture was refluxed at 413 K for 6 h, the mesoporous Al-MCM-41 material (1.8 g) was added into the hot black mixture, refluxed for 30 min, then phosphoric acid (0.54 g, 85 wt%) was, with controlled ratio of vanadium/phosphorus = 1.0/1.2, added into the mixture. After refluxing for another 6 h, the turbid reaction mixture was filtered and the obtained precipitate, which was typically defined as the supported VPO catalysts precursor, was dried in air at 393 K for 24 h. The catalyst precursors with other loadings were prepared in the same way.

2.3. Characterization

X-ray diffraction patterns were collected at room temperature using a Shimadzu XD-3A diffractometer with graphite-filtered Cu Kα radiation. Nitrogen adsorption isotherms were measured on a Micromeritics ASAP2000 apparatus. Surface areas were calculated according to the BET theory, and the pore size distribution was calculated using the BJH method. XPS was performed on an X-ray photoelectron spectrometer – VG ESCALAB MKII, with the X-ray (Mg Kα) energy of 1253.6 eV and the set vacuum less than 2×10^{-8} mbar. The binding energies were normalized based on the C 1s value of 284.6 eV. The particle size of the samples was examined on a TEM-200CX transmission electron microscope (TEM). Temperature-programmed reduction (TPR) experiments were executed in the H_2/N_2 mixture (5 : 95 v/v, flow rate 20 ml/min), at a rate of 5 K/min from room temperature to 873 K. Analysis of hydrogen consumption was accomplished using a thermal conductivity detector. Water, evolved during reduction, was removed from the gas stream using a cold trap.

2.4. Performance testing

All the *in situ* activated catalyst samples were tested for partial oxidation of *n*-butane in the temperature range of 573–733 K. A quartz microreactor was loaded with a 0.5 g granulated sample, and 1.5% *n*-butane/air mixture was introduced at the gas hourly space velocity (GHSV) of 1200 h^{-1}. On-line gas chromatography systems were used to analyze the outlet mixture, and the carbon balance was generally better than 95%.

3. Results and discussion

3.1. Characterization of the VPO specimen supported on mesoporous Al-MCM-41

Figure 1 shows the XRD patterns of the Al-MCM-41 supported VPO catalysts with different vanadium loading after activation as well as the pure Al-MCM-41 support after calcination. It was found that the support showed the typical hexagonal structure corresponding to that reported earlier by Beck *et al.* [10]. After supporting VPO, the diffraction

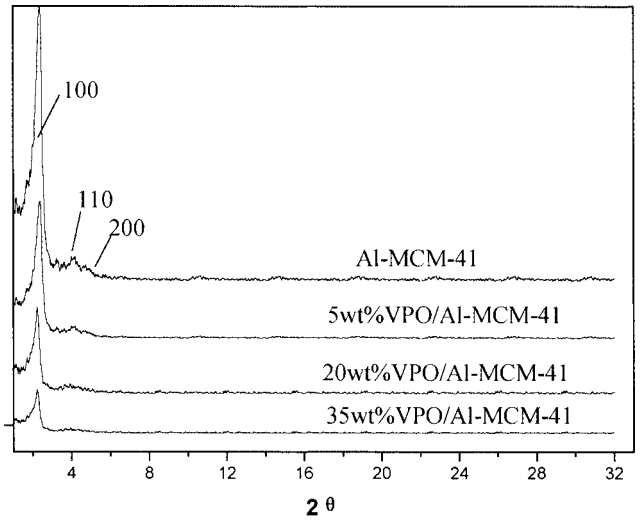

Figure 1. XRD patterns for the Al-containing MCM-41 supported VPO samples after activation.

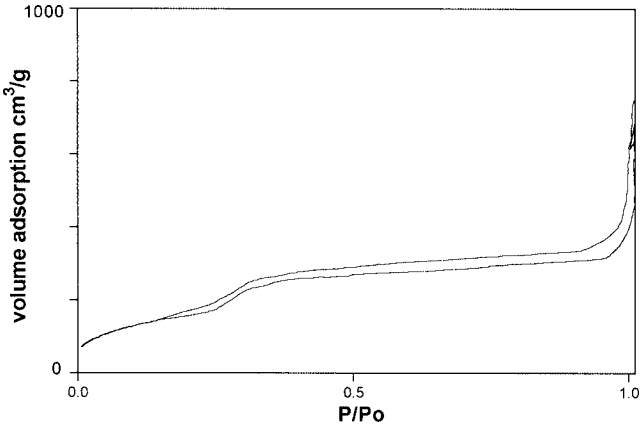

Figure 2. N_2 adsorption–desorption isotherm obtained on the 20 wt% VPO/Al-MCM-41 sample.

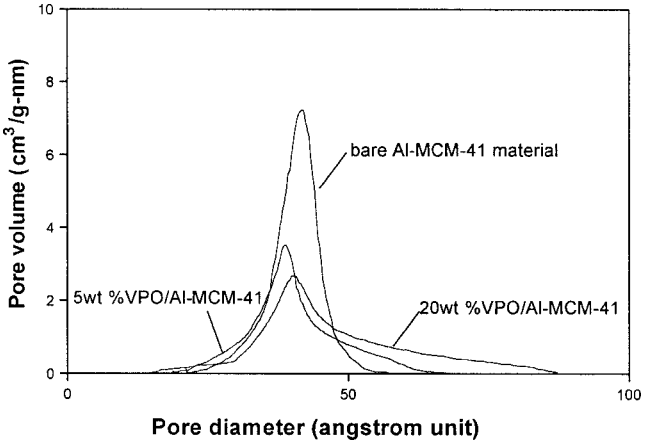

Figure 3. Pore-size distributions of the Al-MCM-41 supported VPO catalysts and the corresponding Al-MCM-41 support.

patterns displayed are only the characteristics of the support, and no VPO crystallite can be observed even for the 18.6 wt% loading of vanadium. Most of the supported VPO species could be in amorphous form and dispersed in the internal channels as well as on the external surface. Ruitenbeek *et al.* early reported that on the SiO_2 supported VPO catalysts the VPO species was also in amorphous state [15]. Very recently, Hutchings *et al.* claimed that even the unsupported amorphous VPO prepared through SCFD in CO_2 was nearly as active as its crystalline counterpart [16]. The VPO species present had a notable effect on the intensity and width of the main d_{100}-spacing, and the peak becomes broader and weaker with the increasing loading, which suggested that the long-range order of the Al-MCM-41 was decreased noticeably by the presence of VPO species. In order to evaluate the surface areas and the porosity of the supported materials, N_2 adsorption was applied to the samples. The N_2 adsorption–desorption isotherm for the 20 wt% VPO/Al-MCM-41 sample is shown in figure 2 as an example, and the pore-size distribution curves are presented in figure 3. The data of surface areas and the average pore sizes are given in table 1. For all the samples, the isotherms showed the similar inflection feature around $P/P_0 = 0.2$–0.3, which was the characteristic of mesoporous materials with uniform pore size [10].

Table 1
Physical characteristics of the catalysts with Si/Al = 30, P/V = 1.2.

Catalyst sample	Average pore size (Å)	S_{BET} (m^2/g)
Pure MCM-41	38.4	887
5 wt% VPO/MCM-41	33.7	648
20 wt% VPO/MCM-41	36.0	452
35 wt% VPO/MCM-41	38.0	383

As can be seen in table 1, the specific surface areas of the supported catalysts were appreciably lower than that of the pure Al-MCM-41 support. The loading of VPO had an obvious impact on the overall surface area, which decreased with increasing VPO loading. Interestingly, the average pore size was increased with increasing VPO loading, as can be seen more clearly in table 1. On the higher loading samples, it is possible that much more pores are plugged by the supported component around the pore mouth, resulting in those pores being no longer accessible for nitrogen adsorption and consequently a significant decrease in specific surface area. Moreover, some larger pores were generated on the higher loading sample, which could be due to the more pronounced structural and textural changes of the MCM-41 support, as also revealed in the XRD results. On the whole, the apparent average pore size on the higher loading sample was less changed. On the lower loading sample, however, more VPO species were present inside the pores, resulting in a smooth decrease in both the surface area and the pore-size distribution. From figure 3, it seems unlikely that the active phase is precipitated next to the support, since, if this occurred, a bimodal pore size distribution would be expected, but this was not observed. Therefore it was thought that the supported vanadium–phosphorus oxide species were presumably dispersed on the support surface, which is in agreement with the XRD observations. Transmission electron microscopy (TEM) examination also revealed that in the low loading sample the supported VPO component could be well-dispersed on the support surface and was hardly distinguished from the support images, while in the high loading sample some VPO components, presumably in amorphous form, are present around the pore mouths and on the external support surface, as shown in figure 4 (a) and (b), respectively.

The data of XPS measurements on the Al-MCM-41 supported VPO catalysts are summarized in table 2. The fresh Al-MCM-41 supported VPO catalysts activated *in situ* at 673 K for 6 h as well as a used one were included. It was revealed that the support surface was covered by VPO species since the vanadium and phosphorus signals were detected in all cases and it was also reflected by the change of surface Si/V ratios with the VPO loading. For the used sample, although the P/V ratio basically retained, the surface Si/V ratio notably decreased. This implies that there might be a structural rearrangement of the supported VPO species under reaction condition [17]. It was also found that the P element

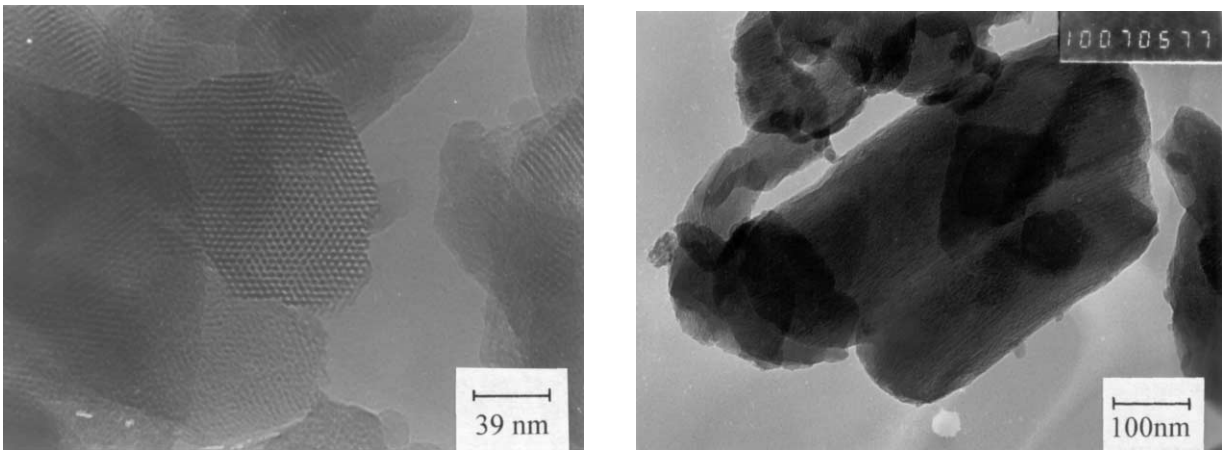

(a) (b)

Figure 4. Representative TEM graphs of the activated Al-MCM-41 supported samples: (a) 5 wt% loading sample, and (b) 20 wt% loading sample.

Table 2
V $2p_{3/2}$ binding energies and P/V and Si/V ratios determined by XPS.

Catalyst sample	V $2p_{3/2}$ (eV)	Atomic ratio	
		P/V	Si/V
5 wt% VPO/MCM-41 (activated at 673 K for 6 h)	516.8	1.5	17.8
20 wt% VPO/MCM-41 (activated at 673 K for 6 h)	517.0	2.9	11.4
35 wt% VPO/MCM-41 (activated at 673 K for 6 h)	517.6	3.1	9.1
5 wt% VPO/MCM-41 (after reaction)	517.1	1.3	12.5

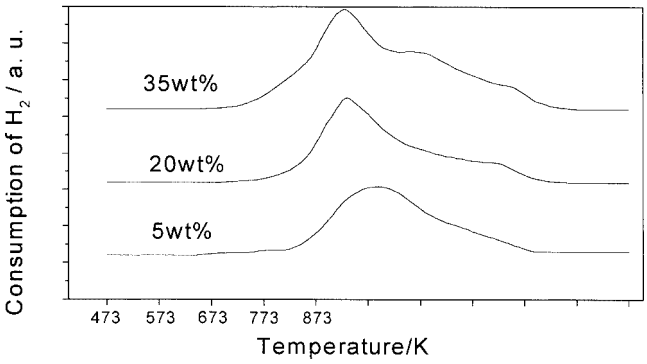

Figure 5. TPR profiles of the Al-MCM-41 supported VPO catalysts with different loadings.

was enriched on the surface, which is the common phenomenon observed on the unsupported VPO catalysts [18,19]. The surface P enrichment was thought to be favorable to improve the MA selectivity for the butane oxidation on the unsupported VPO catalyst [20], but in our case, there was no clear relationship established between these two parameters and it will be discussed below. Note that the degree of surface P enrichment becomes more pronounced on the higher loading samples, suggesting the state of supported VPO species varied somewhat with increasing loading, which in turn affects the interaction between the VPO species and the MCM-41 support. As for the binding energies of vanadium, the values are close to that reported for $(VO)_2P_2O_7$, namely, 517.6 eV [20], but notably lower than that for V_2O_5 [22] and β-$VOPO_4$ [20]. Therefore, the average oxidation state of vanadium in these supported samples should be around 4+. Note that the binding energy of vanadium increased with increasing loading, and the largest deviation was up to 0.8 eV, which clearly indicated that the interaction between the supported component and the support varied with loading.

Figure 5 shows the reduction behavior of the Al-MCM-41 supported catalysts with different loadings. Since the support itself was not reduced in the applied temperature range, the observed reducibility should be attributed to the supported VPO species, mostly in surface regions due to relatively low reduction temperatures applied. It seems that the reducibility increased with increasing vanadium loading. De Boer made a similar observation on the silica supported MoO_3 catalysts at the loading of 3–9 wt% MoO_3 [23]. He suggested that the low reducibility could be due to the well-dispersed MoO_3 species on the support surface. In our case, it is possible that the dispersion state also has an impact on the reduction of the supported VPO species. It is suggested that the interaction of the VPO specimen with the Al-MCM-41 support surface might lead to part of oxygen atoms shared between (surface) Si and V atoms at the border of the well-dispersed VPO cluster and the Al-MCM-41 support surface, which could result in apparently low reactivity and reducibility of lattice oxygen. Actually, it was found that the on-set temperature of reduction of the Al-MCM-41 supported catalysts shifted to lower temperatures with increasing loadings. From these results, it is clear that the nature of the interaction between the applied VPO species and the support could be varied with VPO loading and likewise affected the reduction behavior of the related lattice oxygen atoms.

3.2. Reaction performance in selective oxidation of n-butane

Figure 6 (a) and (b) shows the catalytic performances as a function of reaction temperature over the samples with different vanadium loading. Since the Al-MCM-41 support

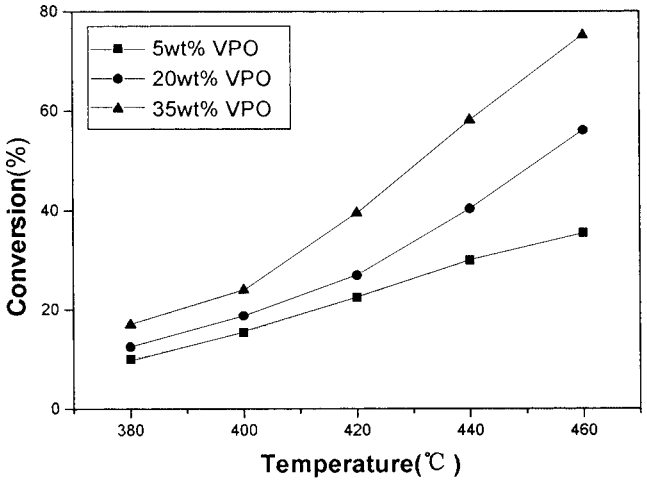

(a)

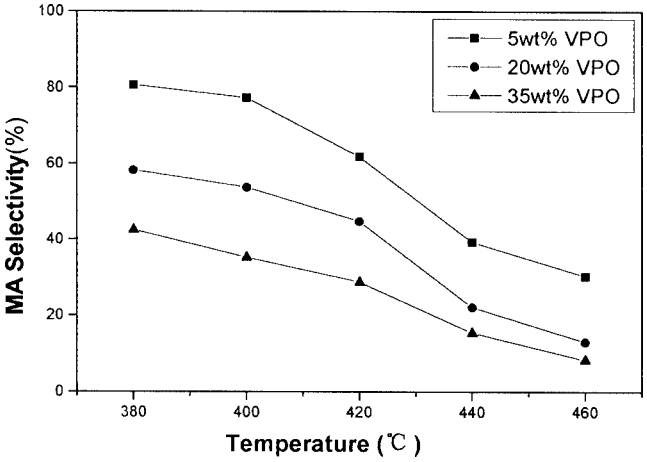

(b)

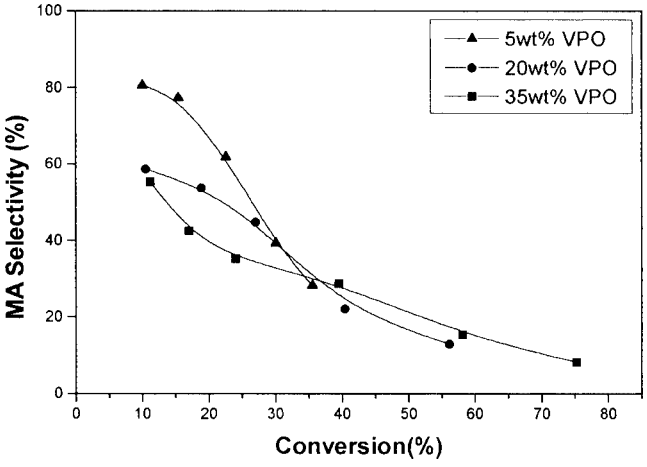

(c)

Figure 6. (a) Conversion and (b) selectivity as a function of reaction temperature, and (c) selectivity as a function of conversion on the supported VPO catalysts.

materials did not show any detectable activity for *n*-butane oxidation under the same experimental conditions, the activity measured should be merely attributed to the supported VPO species. For a further comparison, another supported VPO sample, that is, a 5 wt% VPO loading on the large pore amorphous SiO_2, was prepared and then evaluated under the same reaction conditions.

In figure 6 (a) and (b), it was found that at the same reaction temperature *n*-butane conversion increased while MA selectivity significantly decreased with increasing vanadium loading. It appears that below 673 K both butane conversion and MA selectivity changed slowly, while beyond 673 K they changed sharply at elevated temperatures. The high level of conversion at higher loading probably originated from the more reactive but relatively non-selective active sites present on VPO species loosely interacting with the MCM-41 base. If the selectivity was plotted as a function of the conversion, seen in figure 6(c), it was found that much higher MA selectivity can be achieved at lower conversions (<30%) on the lower loading sample. MA selectivity decreased with increasing conversion and similar level of selectivity would be achieved on different loading samples as butane conversion was beyond 35%. For the SiO_2 supported sample, the typical reaction data obtained at 673 K are *ca.* 44% conversion and 38% MA selectivity (not shown in the figure). Clearly, a distinctive reaction behavior was observed between these two kinds of supported samples.

As discussed in the previous sections, the interaction between the active VPO species and the support changed with different loading, which affected the related structural feature and the reactivity of lattice oxygen. Bueno *et al.* reported that the $VO(SiO)P_2O_7$ phase could form in SiO_2 supported VPO samples, especially when prepared in inorganic medium [24]. It is likely that the VPO species present predominately in the hexagonal pores on the lower loading sample have a proper interaction with the MCM-41 support, which is beneficial to MA formation. Furthermore, the incorporated Al^{3+} in the framework of MCM-41 support may function more evidently to the surface acidity of support at low loading, which also has an impact on MA selectivity. On the other hand, a quick drop in selectivity at high butane conversion on the low loading sample may, then, be attributed to the much higher reaction temperature requested for attaining the conversion.

4. Conclusions

Al-containing MCM-41 supported VPO catalysts with different vanadium loadings have been synthesized for the first time for the partial oxidation of butane to MA. The MCM-41 support material still basically maintained the ordered hexagonal structure. The supported VPO component was found to be mostly in amorphous form. The resulting VPO species was anchored to the support material. Phosphate element was enriched on the sample surface and the degree of enrichment increased with increasing loading. A possible redispersion of the VPO species may occur during the reaction procedure.

The reactivity as well as the reducibility of the supported VPO species, as deduced from the consumption of H_2, notably changed with VPO loading. The structural feature of the VPO species and the interaction between the VPO

species and the support remarkably altered with loading, which determined the reduction behavior of the supported catalysts.

For the same reason, both butane conversion and MA selectivity are apparently closely related to the loading. At low conversions (<30%), the selectivity increased with decreasing loading, but inversely at higher conversions. The inherent relationship among the loading, the dispersion state, the structural feature of the supported species, and the interaction between the VPO species and the support determined the overall catalytic performance. Although the depth of the relationship between the different variables on the catalytic chemistry has not yet been fully recognized, the concept of applying vanadium–phosphorus oxide onto the mesoporus Al-MCM-41 provided a new and alternative approach for its appropriateness to help to understand the complexity of catalytic chemistry of VPO catalysts.

Acknowledgement

The financial support (grant no. 2000048009) from the Ministry of Science and Technology of China is greatly appreciated.

References

[1] G. Centi, F. Trifirò, J.R. Ebner and V.M. Franchetti, Chem. Rev. 88 (1988) 55.
[2] K.E. Birkeland, S.M. Babitz, O.K. Bethke, H.H. Kung, G.W. Coulston and S.R. Bare, J. Phys. Chem. B 101 (1997) 6895.
[3] R.A. Overbeek, A.R.C.J. Pekelharing, A.J. van Dillen and J.W. Geus, Appl. Catal. A 135 (1996) 231.
[4] R.A. Overbeek, P.A. Warringa, M.J.D. Combag, L.M. Visser, A.J. van Dillen and J.W. Geus, Appl. Catal. A 135 (1996) 209.
[5] V.A. Zazhigalov, Yu.P. Zaitsev, V.M. Belousov, B. Partitz, W. Hanke and G. Ohlmann, React. Kinet. Catal. Lett. 32 (1986) 209.
[6] W.D. Harding, K.E. Birkeland and H.H. Kung, Catal. Lett. 28 (1994) 1.
[7] G.J. Hutchings, A. Desmartin-Chomel, R. Olier and J.C. Volta, Nature 368 (1994) 41.
[8] E. Bordes, Catal. Today 1 (1987) 499.
[9] C.T. Kresge, M.E. Leonowicz, WJ. Roth, J.C. Vartuli and J.S. Beck, Nature 359 (1992) 710.
[10] J.S. Beck, L.C. Vartuli, WJ. Roth, M.E. Leonowicz, C.T. Kresge, K.D. Schmitt, C.T.W. Chu, D.H. Olson, E.W. Sheppard, S.B. McMullen, J.B. Higgings and J.C. Schlenker, J. Am. Chem. Soc. 114 (1992) 10834.
[11] J.Y. Ying, *Mesoporous Molecular Sieves*, Stud. Surf. Sci. Catal., Vol. 117 (Elsevier, Amsterdam, 1998) p. 85.
[12] J. Ramirez, R. Contreras, P. Castillo, T. Klimova, R. Zarate and R. Luna, Appl. Catal. A 197 (2000) 69.
[13] V.V. Guliants, Catal. Today 51 (1999) 255.
[14] A. Corma, V. Fornes, M.T. Navarro and J. Perez-Pariente, J. Catal. 148 (1994) 569.
[15] M. Ruitenbeek, A.J. van Dillen, A. Barbon, E.E. van Faassen, D.C. Koningsberger and J.W. Geus, Catal. Lett. 55 (1998) 133.
[16] G.J. Hutchings, J.K. Bartley, J.M. Webster, J.A. Lopez-Sanchez, D.J. Gilbert, C.J. Kiely, A.F. Carley, S.M. Howdle, S. Sajip, S. Caldarelli, C. Rhodes, J.C. Volta and M. Poliakoff, J. Catal. 197 (2001) 232.
[17] R.A. Overbeek, M. Versluijs-Helder, P.A. Warringa, E.J. Bosma and J.W. Geus, Stud. Surf. Sci. Catal. 82 (1994) 183.
[18] P. Delichere, K.E. Bere and M. Abon, Appl. Catal. A 172 (1998) 295.
[19] F. Garbassi, J.C.J. Bart, R. Tassinari, G. Vlaic and P. Langarde, J. Catal. 98 (1986) 317.
[20] S.K. Hodnett, Catal. Rev. 27 (1985) 373.
[21] H. Igarashi, K. Tsuji, T. Okuhara and M. Misono, J. Phys. Chem. 97 (1993) 7065.
[22] V.I. Bukhtiyarov, Catal. Today 56 (2000) 403.
[23] M. De Boer, Ph.D. thesis, Utrecht University (1992).
[24] J.M.C. Bueno, G.K. Bethke, M.C. Kung and H.H. Kung, Catal. Today 43 (1998) 101.